

Damping of subsynchronous resonance using a voltage source converter-based high-voltage direct-current link in a series-compensated Great Britain transmission network

Luke Livermore¹, Carlos E. Ugalde-Loo¹, Qing Mu², Jun Liang¹, Janaka B. Ekanayake¹, Nick Jenkins¹

¹School of Engineering, Institute of Energy, Cardiff University, Queen's Buildings, The Parade, Cardiff, Wales CF24 3AA, UK

²Power System Department, China Electric Power Research Institute, 15 Xiaoyingdonglu, Haidian, Beijing 100192, People's Republic of China

E-mail: Ugalde-LooC@cardiff.ac.uk

Abstract: Owing to increased levels of generation in Scotland, substantial onshore and offshore reinforcements to the Great Britain (GB) transmission network have been proposed. Possible inland reinforcements include the use of series compensation through fixed capacitors. This potentially can lead to subsynchronous resonance (SSR). Offshore reinforcements are proposed by high-voltage direct-current (HVDC) links. In addition to its primary functions of bulk power transmission, a voltage source converter-based HVDC link can be used to provide damping against SSR, and this function has been modelled. Simulation results have been carried out in Power Systems Computer-Aided Design, with system analysis conducted in MATLAB. A real-time hardware-in-the-loop real-time digital simulator-HVDC test rig has been used to implement and validate the proposed damping scheme on an experimental platform. The simulation and experimental results show good agreement.

Nomenclature

AI	analogue input
AO	analogue output
BNC	Bayonet Neill-Concelman (connector)
BPF	band-pass filter
dSPACE	Digital Signal Processing and Control Engineering
EMTDC	Electro-Magnetic Transients for DC
FACTS	flexible AC transmission systems
FC	fixed capacitor
GB	Great Britain
GPC	gigahertz processor card
HVDC	high-voltage direct-current
NETS-SQSS	National Electricity Transmission System – Security and Quality of Supply Standard
PLL	phase-locked loop
PSCAD	Power Systems Computer Aided Design
RTDS	Real-Time Digital Simulator
SSR	subsynchronous resonance
STATCOM	static synchronous compensator
SUB	subsynchronous mode
SUPER	supersynchronous mode
TCSC	thyristor-controlled series compensator
TM _x	<i>x</i> -th torsional mode
VSC	voltage source converter

1 Introduction

Increased generation in Scotland, in addition to the existing large thermal and nuclear generators that are close to the Anglo-Scottish intertie, has brought operational challenges to the Great Britain (GB) network. The transmission of the additional power from Scotland to England is currently constrained by stability limits and thermal ratings [1]. The Electricity Networks Strategy Group, in its 2020 Vision, has proposed substantial circuit reinforcements and deployment of new technologies to strengthen the existing Anglo-Scottish intertie and to increase the transfer capacity of the Scotland–England transmission boundary [1, 2]. The onshore reinforcement includes the installation of series compensation in the form of fixed capacitors (FCs). As an offshore reinforcement, submarine high-voltage direct-current (HVDC) links have been specified.

The presence of series compensation in the GB system will not only alter line characteristics and their transient behaviour, but could also bring potential subsynchronous resonance (SSR) [3]. SSR is an electric power system condition where the electric network exchanges energy with a turbine generator at one or more of the natural frequencies of the combined system below the synchronous frequency [4, 5]. This phenomenon mainly occurs in series capacitor-compensated transmission networks. If an

interaction between the natural frequencies of the electrical network and of a turbogenerator occurs, subsynchronous oscillations may arise. If appropriate measures are not taken, this can lead to stress, fatigue and damage to the turbine shaft [6, 7]. SSR has been well documented in the past [4–8]. Shaft failure and damage on turbogenerators connected to series-compensated transmission lines have been traced to SSR [6, 9].

Although the SSR phenomenon is not new, it has been observed predominantly in countries with long transmission lines and relatively low fault levels [3, 7]. The GB network is more tightly meshed with high fault levels. The GB system has large thermal and nuclear generation near the Anglo-Scottish intertie (e.g. at Torness, Heysham, Hunterston, Hartlepool), and so the effect of series compensation needs to be evaluated within this context. This is currently a topic of high industrial and academic interest [1–3].

The occurrence and damping of SSR in a series-compensated GB transmission network was examined both through a real-time implementation and computer simulations. A three-machine model, resembling the operating conditions of the mainland GB system, was studied. Although simple in nature, the network features an appropriate weighting of the size and type of generation, which is representative of a projected GB operating condition. This model was obtained in consultation with the GB transmission system operator (National Grid Ltd) and has been previously used in research studies [10]. The system has been modified to include both onshore and offshore reinforcements in the form of series capacitors and a voltage source converter-based HVDC (VSC-HVDC) link. Besides providing bulk power transmission, the VSC-HVDC link has an auxiliary control loop designed to damp SSR.

SSR mitigation has been a topic of research interest over several years [4, 7]. Several countermeasures have been proposed, ranging from limiting levels of series compensation through system planning, filtering, damping schemes and the use of FACTS devices [6, 11–14]. In particular, the thyristor-controlled series compensator (TCSC) has the capability to damp SSR [15]. By controlling the firing angle of thyristors, the effective reactance of the TCSC can be modified, together with the electrical resonant frequency of the compensated line. Through a careful selection of the boost factor, the TCSC equivalent impedance at subsynchronous frequencies can exhibit an inductive behaviour with a strong resistive component, reflecting in SSR damping while providing the necessary level of series compensation [16, 17].

Although the TCSC provides an alternative to conventional series compensation using FCs, its use requires additional primary plant, higher capital costs and a larger space. Instead, SSR can be damped using the VSC-HVDC link that is already proposed [2]. This approach has the following additional advantages:

- (1) VSC-HVDC links can operate as STATCOMs and thus provide SSR damping following a failure in the DC transmission line [13].
- (2) HVDC bi-poles are often operated as independent monopoles to satisfy National Electricity Transmission System Security and Quality of Supply Standard (NETS SQSS) requirements [18], so one should always be active and thus, providing damping.
- (3) In case of failure of one converter, the other terminal can still provide SSR damping.

- (4) In the unlikely case that the VSC-HVDC link becomes inoperable, the transfer capacity of the AC connection will be reduced but not lost, with the series compensation being restricted to a safe level.

Given the high costs associated with building VSC-HVDC links, the availability of the entire link is very high (>95%) [19]. In addition, the NETS SQSS requires that a maximum loss of 1.3 GW is allowed [18]; as the proposed link is greater than this value, the link will have to operate with redundancy. Moreover, following any fault in the bi-pole the link will operate as a monopole and will remain online, albeit at a reduced capacity. On the other hand, a TCSC will only be active as long as the AC line is in service.

The use of a SSR damper embedded in the VSC-HVDC link controller has been previously examined in the literature [20, 21]. In general, it consists of gains, washout filters and lead-lag compensators to appropriately damp troublesome torsional modes. The damping strategy proposed in this paper measures the subsynchronous currents in the AC system and uses this information to generate a damping signal which mitigates SSR.

The main contributions of this paper are the validation and implementation of an auxiliary SSR damping loop embedded in the control scheme of a VSC-HVDC link. This has been developed on a hardware-in-the-loop real-time experimental platform, which has been assembled to provide a test-bench for dynamic studies of a reinforced GB system. A Real-Time Digital Simulator (RTDS) has been used to model the AC system. Although a simplified network representation has been employed, the experimental platform validated and reported in this paper has the flexibility to incorporate models of the generators and transmission network of more complex systems. The analytical, simulation and experimentation tools developed here allow the generator and transmission system operators to assess the impacts of series compensation, the SSR phenomenon and the use of the parallel VSC-HVDC link to mitigate it.

Since there is no data available in the open literature of GB turbine-generator shafts, typical generator plant data were used. The studies presented here demonstrate a methodology for designing an SSR damper using system information found in the literature. The proposed damping scheme has been assessed both through simulations and formal analysis. The task of implementing such a damper in practice is relatively simple given accurate AC system data. If available, more appropriate data could be incorporated easily into the RTDS model used here.

The remainder of the paper is organised as follows: Section 2 presents series compensation as an onshore reinforcement of the GB transmission network. A three-machine system specifically designed to study SSR in GB is introduced, together with an eigenanalysis carried out in MATLAB to characterise SSR in such a system. Section 3 addresses offshore reinforcements in the form of HVDC-links and their control. An auxiliary controller to damp SSR is presented, together with simulations performed in the Electro-Magnetic Transients for DC/Power Systems Computer Aided Design (EMTDC-PSCAD) engine to show the controller performance. The experimental platform, consisting of an RTDS and a VSC-HVDC test rig, is described in Section 4. Section 5 presents the results obtained through real-time experiments carried out in the multi-platform network, demonstrating the feasibility of the damping strategy and validating the simulation results from Section 4. The conclusions given in Section 6 end the paper.

2 Onshore reinforcement through fixed capacitors

Series compensation has been predominantly used to decrease the electrical length of long transmission lines [7]. However, the GB transmission system is a compact and meshed network in which series compensation has not been previously used. Although FCs will increase transient stability limits, the presence of a large number of thermal generators in proximity to the series-compensated Anglo-Scottish intertie introduces the risk of SSR [3].

The three-machine network introduced in [10], originally designed to resemble the operating conditions of the mainland GB system, has been adapted to include series compensation and a VSC-HVDC link [22, 23]. This is shown in Fig. 1. Although it depicts a simplified case study of the British network, the model provides a clear understanding of the SSR phenomenon. The system splits the GB mainland system into three major generation areas: England/Wales, Southern Scotland and Northern Scotland. The rating of the England/Wales generator is 21 000 MVA, with the Scottish generators having a considerably smaller capacity of 2800 and 2400 MVA, respectively [10]. A series capacitor has been included between Buses 4 and 5 to represent the series compensation of transmission lines between England and Scotland. All system parameters are given in [23] and included in Appendix 1 for completeness.

To assess the occurrence of SSR, the shaft of the Northern Scotland generator was modelled as a multi-mass system as in [8]. This consists of a tandem-compound steam turbine, where the rotor sections are all on one shaft [6, 7]. The shaft parameters given in [8] were used to represent aggregated steam turbines located in Northern Scotland as there is no available data of GB generator shafts in the open literature. The remaining two generators have a single-mass shaft representation. The three-machine system is described by a set of differential equations, linearised around an operating point. The system has been constructed in MATLAB to perform eigenanalysis.

The series-compensated system shown in Fig. 1 is characterised by four unstable torsional modes (TM1–TM4) associated with the shaft of the Northern Scotland generator which may be excited at different levels of compensation [23]. As it can be seen in Fig. 2, system stability is directly related to the subsynchronous mode of the transmission line connected to the Northern Scotland generator (termed SUB), whose frequency decreases as the percentage of series compensation increases. Stability is lost whenever the frequency of SUB is in the neighbourhood of a TM frequency, as reflected by the positive real part of the eigenvalues of TM1–TM4 under such conditions.

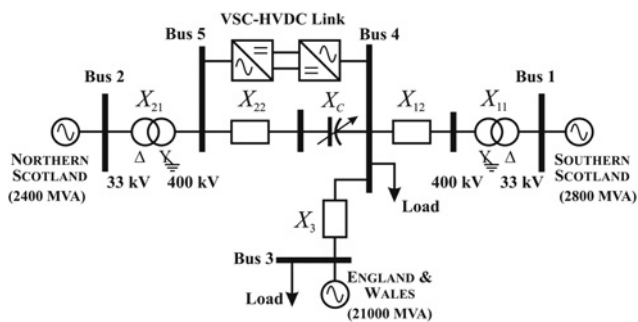


Fig. 1 Three-machine network with onshore and offshore reinforcements through series capacitors and a VSC-HVDC link

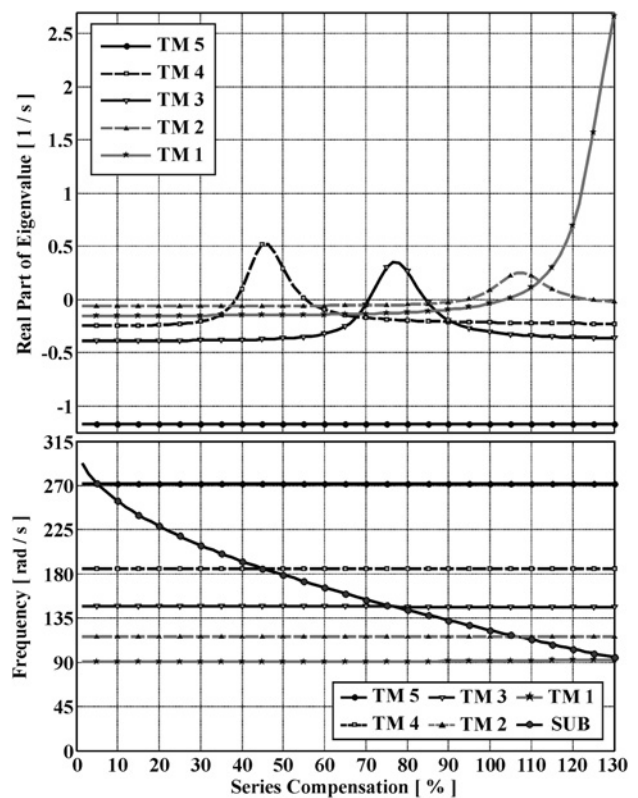


Fig. 2 Stability of the torsional modes in terms of series compensation [23]

Although additional subsynchronous modes exist in the network due to RL branches associated with loads and transmission lines connecting the England/Wales and Southern Scotland generation, they do not interact with the TMs of the Northern Scotland generator. This has been confirmed through eigenvalue and participation factor analyses carried out in [23]. For further information on system modelling, the reader is referred to [24], where the complete state-space representation of the synchronous generator with a multi-mass shaft is provided.

Table 1 summarises the relevant eigenvalues for 30 and 40% series compensation of the transmission line connecting the Northern Scotland generator and Bus 4. As it can be seen, when 30% of compensation is employed the system is stable. However, for 40% the SUB mode (≈ 30.7 Hz) interacts with TM4 of the shaft (≈ 29.6 Hz). As a consequence, SSR arises and TM4 becomes unstable.

The analysis presented in this section focuses on a particular type of SSR, torsional interactions – described in detail in [4, 5], which is a consequence of the interplay between electrical and mechanical systems. Other types of SSR (i.e. induction

Table 1 Relevant eigenvalues of the three-machine system

Mode of oscillation	30% compensation		40% compensation	
	Real part, s ⁻¹	Imag. part, rad/s	Real part, s ⁻¹	Imag. part, rad/s
TM5	-1.173	±272.1935	-1.173	±272.1935
TM4	-0.2078	±185.4883	+0.0976	±185.7151
TM3	-0.3839	±146.6666	-0.3792	±146.6967
TM2	-0.0587	±115.9705	-0.0584	±115.9755
TM1	-0.1492	±90.5749	-0.1475	±90.6216
SUPER	-8.5183	±418.5203	-8.6653	±434.764
SUB	-7.4436	±209.2895	-7.6743	±192.7548

generator effect, transient torques, subsynchronous control interactions) [4, 5, 25] are out of the scope of this paper.

3 Offshore reinforcement through HVDC links

Reinforcement of the British network is a compromise between the difficulty in building new inland overhead lines and the risks of using technologies new to the transmission system [22]. According to [2], two HVDC links between Scotland and England/Wales each at a rating of 2.1 GW have been proposed as offshore reinforcements. The Western link is planned to connect Hunterston in Scotland with Deeside in Wales. The Eastern link will connect Peterhead in Scotland with Hawthorne Pit in England. Although line commutated HVDC technology is well established, the emergence of VSC-HVDC [26, 27] provides an alternative transmission technology and is a candidate for one of the links.

In [28], a comprehensive study on the role that VSC-HVDC links has on SSR has been presented. Through damping torque and eigenvalue analyses, it has been shown that the impact of the HVDC link on SSR is minimal; in fact, for some operating conditions, it contributes positive damping. Therefore, the presence of the HVDC link, by itself, will not reinforce SSR, as shown by the simulations and experimental results in Sections 3.3 and 5. It should be emphasised that [28] centres the discussion on torsional interactions, which is the type of SSR that this paper addresses.

Comprehensive studies on the different modes of operation of the VSC-HVDC link and its possible interaction with the auxiliary control scheme to damp SSR once series compensation is in place are required. For the purpose of this work, a VSC-HVDC link is connected between Buses 4 and 5 of the three-machine network, as shown by Fig. 1. SSR is stimulated by the series compensation of the AC system.

3.1 Primary control of the VSC-HVDC link

The primary objective of the HVDC link is to ensure that active power control is achieved along with reactive power support for the grid. This approach has been used previously [29, 30] and is shown in Fig. 3. The parameters to be controlled are the active and reactive power at both terminals and the DC link voltage. Reactive power control is specified as this is the control parameter for AC voltage control, power factor control or auxiliary functions such as power oscillation damping. A phase-locked loop (PLL) is used to synchronise the reference frame. For further details on the control scheme and its performance, refer to [22]. Control parameters can be found in Appendix 2.

3.2 Auxiliary controller to damp SSR

To damp SSR, an auxiliary controller has been designed, shown in Fig. 3. Under this control scheme, the VSC terminal A includes a damping controller which injects an anti-phase signal into the AC system at a target subsynchronous frequency. The controller was designed in a dq reference frame to complement the primary control. An alternative strategy might be to use an auxiliary controller directly in an abc reference frame; however, this was not investigated.

The eigenvalue analysis in Section 2 (Table 1) indicates that for 40% series compensation SSR arises. TM4 (~30 Hz) becomes unstable owing to its proximity to the frequency

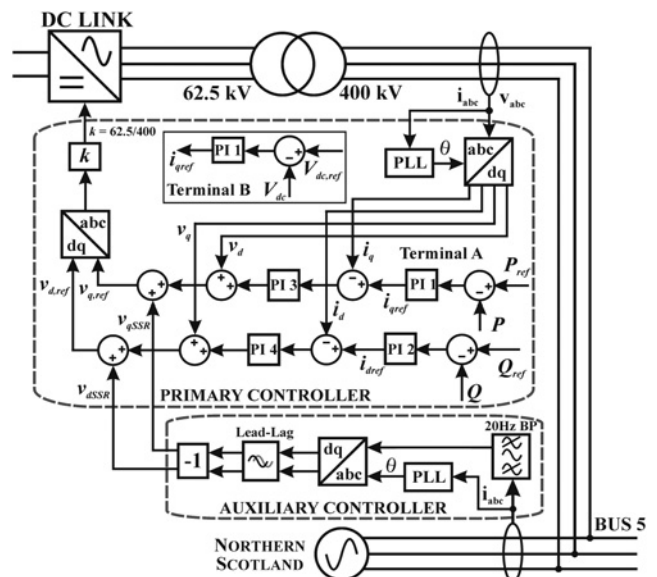


Fig. 3 Primary and auxiliary controllers for SSR damping

of subsynchronous mode SUB. For this case, the damping controller is designed for a target resonant frequency of 20 Hz as this corresponds to the complement frequency of mode SUB [4]. As shown in Fig. 3, a band-pass filter (BPF) isolates the target frequency component, eliminating the voltage driving frequency (50 Hz). The three-phase SSR current is transformed to a dq reference frame through a conversion block, with the reference frame synchronised using a PLL. However, the filtering adds a phase displacement and attenuates the amplitude of the target signal. The lead-lag compensator corrects this. The -1 gain block produces an 180° phase shift to create the SSR damping signal. This gives an anti-phase signal to the original signal and will act to damp SSR on the AC network. The magnitude of the damping signals $v_{d,SSR}$ and $v_{q,SSR}$ is small, in the order of 0.2 kV peak-to-peak. These are then added to the primary control voltage reference (v_d and v_q) 62.5 kV signals. The auxiliary controller operates at a lower bandwidth than the inner primary loops. Damping will only occur when a subsynchronous oscillation is present (i.e. under normal conditions the output of the control loop will be negligible). The apparent current required for SSR damping is 0.02 pu of the apparent current required for primary control. Therefore, any negative effect on the dynamic performance of the system is negligible. All control parameters can be found in Appendix 2.

It can be seen from Fig. 3 that the dq outputs of the auxiliary controller are added to the current loops of the primary control scheme. It could be argued that the converter over-current protection could be compromised under AC faults; however, the performance of the overall control scheme under such contingencies and coordination of protection are out of the scope of this paper. The focus of both simulation and experimental tests is on changes in series compensation only.

3.3 Simulations

Time domain simulations of the system with a VSC-HVDC link (Fig. 1) were carried out on PSCAD, with the results shown in Fig. 4a. The HVDC link primary control strategy was included only. The simulation starts in steady state with a 30% series compensation. At 2 s, the effective value of series compensation is modified to 40%. After such a

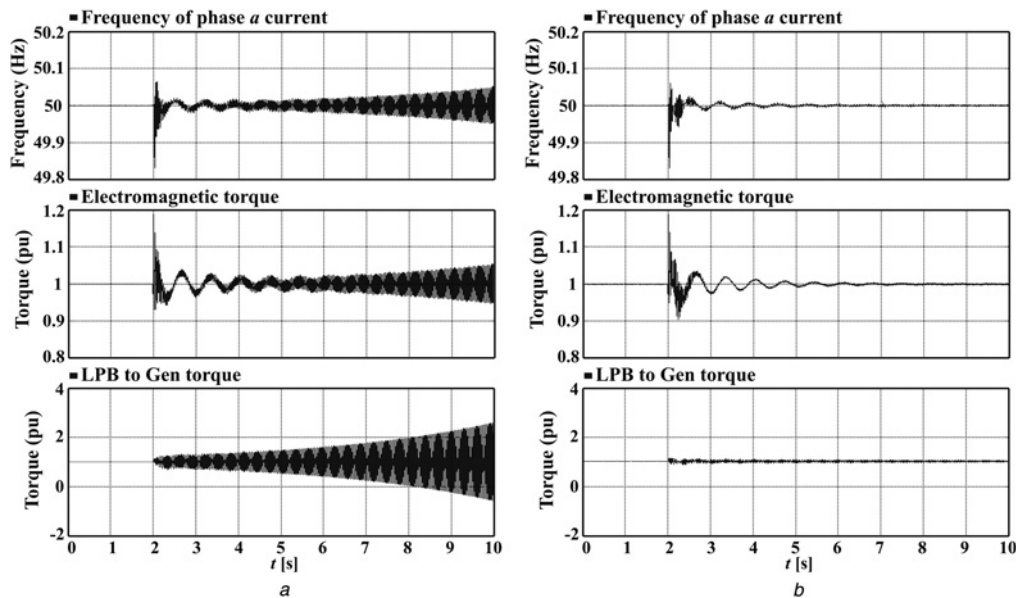


Fig. 4 Simulation results featuring a VSC-HVDC link

a Primary only

b Primary and auxiliary controllers: frequency of phase *a* current, electromagnetic torque, and torque (in the multi-mass shaft between low pressure turbine B and the generator) of the Northern Scotland generator

disturbance, the system develops SSR. As it can be seen, the frequency of the phase *a* current of the Northern Scotland generator presents increasing subsynchronous oscillations. The electromagnetic torque and torque between turbine sections also feature such oscillations. These simulation results are consistent with the information provided by Table 1: SSR was developed at 40% series compensation as no damping countermeasures have yet been taken. Moreover, the effect of the DC link dynamics does not influence the occurrence of SSR.

To test the effectiveness of the auxiliary controller, a similar simulation was carried out with the damping controller being active. The results are shown in Fig. 4*b*. As it can be observed, the proposed auxiliary scheme is able to damp SSR effectively.

Transient simulations were carried out to assess the capability of the auxiliary controller to damp SSR when the interaction with an unstable TM was the maximum and at a reduced load demand, with results shown in Fig. 5. A maximum interaction occurs whenever the SUB mode frequency matches that of a TM, causing the real part of the associated eigenvalue to be a maximum (shown in Fig. 2). Table 2 summarises these interactions as a function of series compensation level. Results with the level of compensation to give a maximum interaction with TM3 and TM4 are obtained and presented in Figs. 5*a* and *b*. As it can be seen, the proposed strategy to damp SSR is effective at different compensation levels. However, the risk of SSR through torsional interaction with TM3 is not expected since less than 40% series compensation is planned in the GB network [3]. The parameters of the damping controller have remained the same in all simulations except for the BPF, which was centred at 27 Hz for a maximum interaction with TM3.

According to [31], the Winter peak load in the UK is twice the value of the Summer low. Thus, for the case of the three-machine network, the value of the loads in [23] was reduced to half their value to represent a Summer day. The results are given in Fig. 5*c*. As can be seen, the damping controller is able to damp SSR under these conditions.

Even though an aggregated generator was used to represent the steam turbines in Northern Scotland, these simulations also show that if the parameters of the BPF are suitably selected the proposed damping strategy is effective for a different turbine. However, demonstrating that SSR could be damped in all generators is beyond the capabilities of the laboratory test rig. Moreover, the simulations presented in this section show that the proposed design method for an auxiliary SSR damping controller is effective over the range of frequencies associated with realistic compensation levels in GB (below 40% [3]), but could include a broader frequency range as shown by Fig. 5. In reality, a 'one-size-fits-all' damper is not possible under the proposed methodology and once appropriate system data becomes available, an SSR study should be carried out as in [23] for every problematic generator individually. An alternative is a damper which filters out the fundamental and damps all other frequencies, although this would be difficult to implement in practice.

4 Experimental platform

The platform used for system implementation, shown in Fig. 6, is based on an RTDS and a three-terminal VSC-HVDC test rig. The test rig consists of three 2 kVA VSCs controlled through a dSPACE unit. The RTDS is a single rack system utilising 4 GPC cards (2 processors per card). The analogue input (AI) and output (AO) terminals were brought to the front of the cabinet to allow BNC connection to the VSC-HVDC rig. Control and hardware parameters for the platform can be found in Appendices 2 and 3.

The experimental design of the network is slightly different to that used for simulations, as shown in Fig. 6*c*. This is due to a limitation in the number of signals which can be exchanged between the RTDS and the VSC-HVDC test rig. However, as it is evident in Section 5, the experimental platform is designed to demonstrate the positive damping effect a VSC converter can have on a connected AC system. The RTDS models the AC network as Section 3, without the HVDC link and a controlled current source was connected to Bus

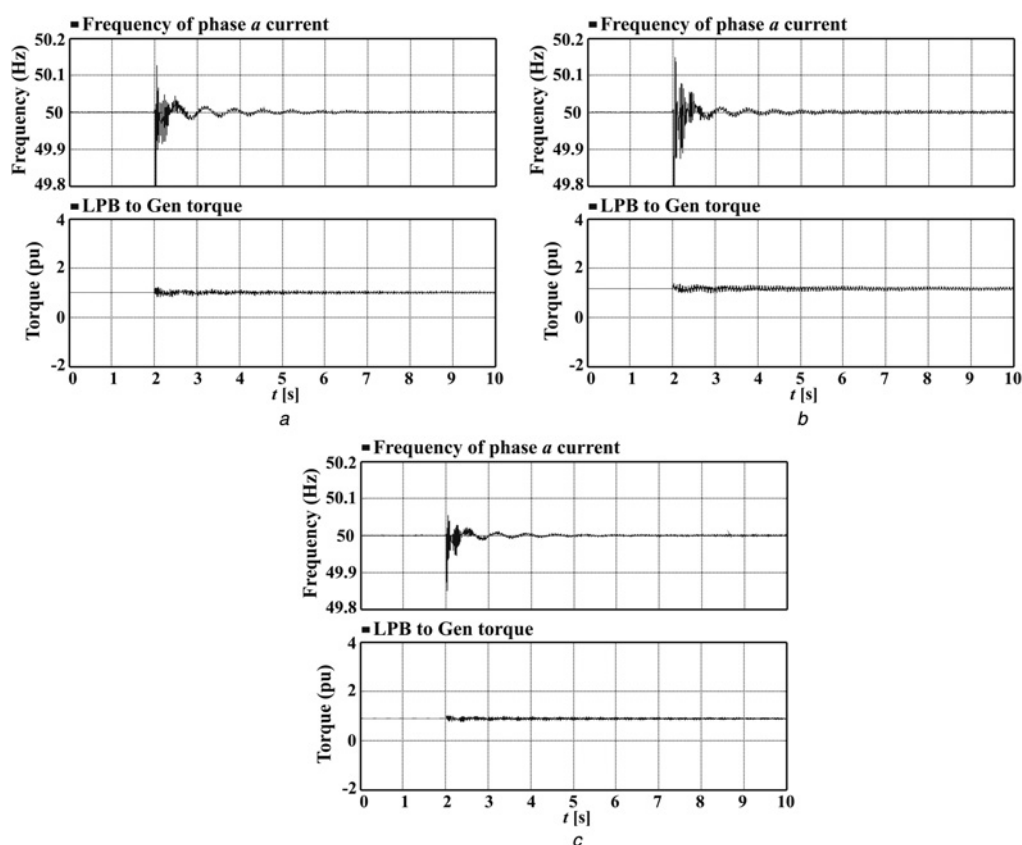


Fig. 5 Assessment of the capability of the auxiliary controller to damp SSR

Frequency of phase *a* current and torque (in the multi-mass shaft between low pressure turbine B and the generator) of the Northern Scotland generator

a Level of compensation to give a maximum interaction with TM4 (45.78% compensation)

b Level of compensation to give a maximum interaction with TM3 (77.15% compensation)

c At a reduced load demand

5. The three terminals of the VSC-HVDC test rig are set up independently. Unlike the simulation, there is no ordered power flow. The damping converter uses both active and reactive power to damp oscillations, with reactive power being dominant. The purpose of each VSC is explained next.

4.1 DC voltage source

To work effectively, the amplifying and damping converters need to operate from a stiff DC voltage. This is provided by a VSC specifically employed to control DC voltage.

4.2 Amplifying converter

The role of the amplifying converter is to establish an AC voltage. This is described by Fig. 7*a*. At the RTDS, the Bus 5 voltages are measured (400 kV) and scaled at the AO card for transmission of the signal to the VSC-HVDC rig

Table 2 Maximum interaction with TMs as a function of series compensation

Mode of oscillation	% comp.	Real part, s^{-1}	Imaginary part	
			rad/s	Hz
TM4	45.78	0.5297	185.4	29.15
TM3	77.15	0.3537	146.6	23.33
TM2	107.37	0.2535	115.97	18.46
TM1	139.59	3.5679	90.5	14.4

(5 V). The amplifying converter is employed to control the AC voltage at its terminals at the nominal voltage for the rig (100 V) using the voltage signal from the RTDS.

4.3 Damping converter

Its role, described by Fig. 7*b*, is to provide the anti-phase current used to damp SSR on the AC system developed on the RTDS. The currents (with SSR) are measured at Bus 5 on the RTDS system. Filtering is achieved through high pass (15 Hz) and low pass (25 Hz) filters to isolate the SSR frequency, removing the system synchronous frequency at 50 Hz. By filtering on the RTDS, the amplitude of the SSR component of the signal can be scaled to the nominal transmission voltage of 5 V at the AO card of the RTDS. This minimises noise issues. A lead-lag compensator is used to correct for the phase shift from the transmission delay. The *dq* current is then transmitted to the HVDC rig. The damping converter receives the transmitted signal, which is a voltage representing a current, before producing an anti-phase current signal. The lead-lag compensator corrects for the phase shift from the filtering, whereas the -1 gain ensures the generated current is anti-phase in relation to the reference signal. The damping converter then generates this signal at its AC terminals. The currents are measured through current sensors on the AC side and sent back to the RTDS (at 5 V) and used as the reference currents to program controllable current sources. These current sources inject the anti-phase current back into Bus 5 on the RTDS.

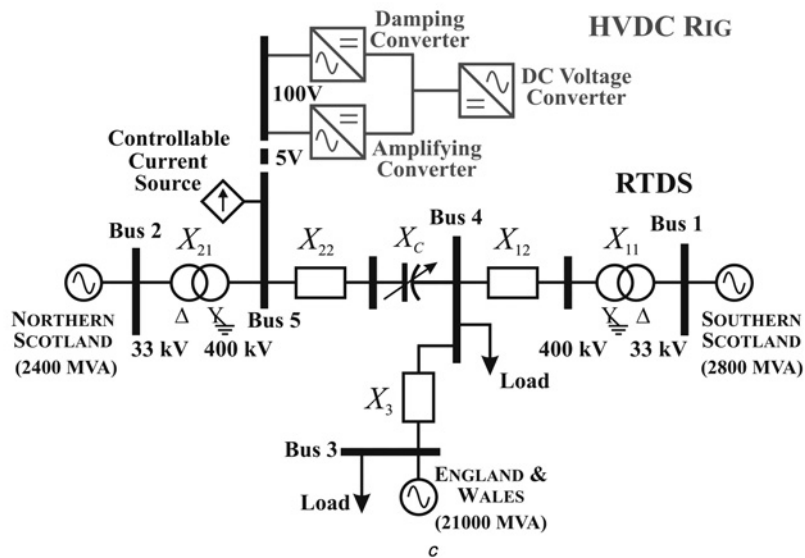


Fig. 6 Experimental platform
 a RTDS
 b HVDC test rig
 c Circuit for experimental design

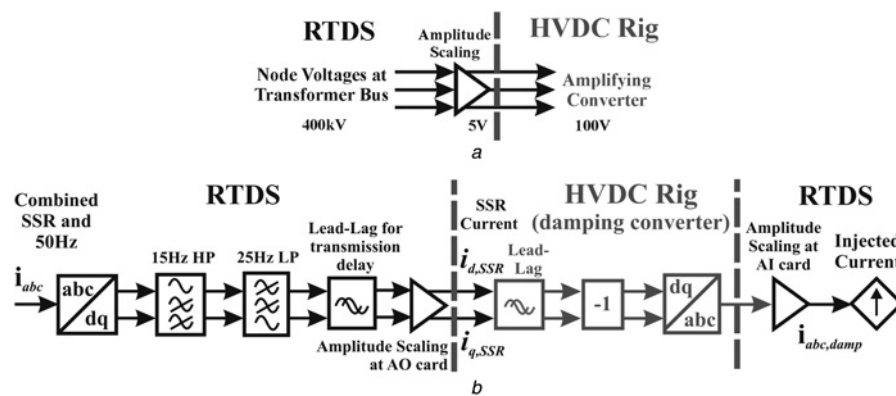


Fig. 7 Signal exchange between the RTDS and the VSC-HVDC test rig
 a Amplifying converter
 b Damping converter

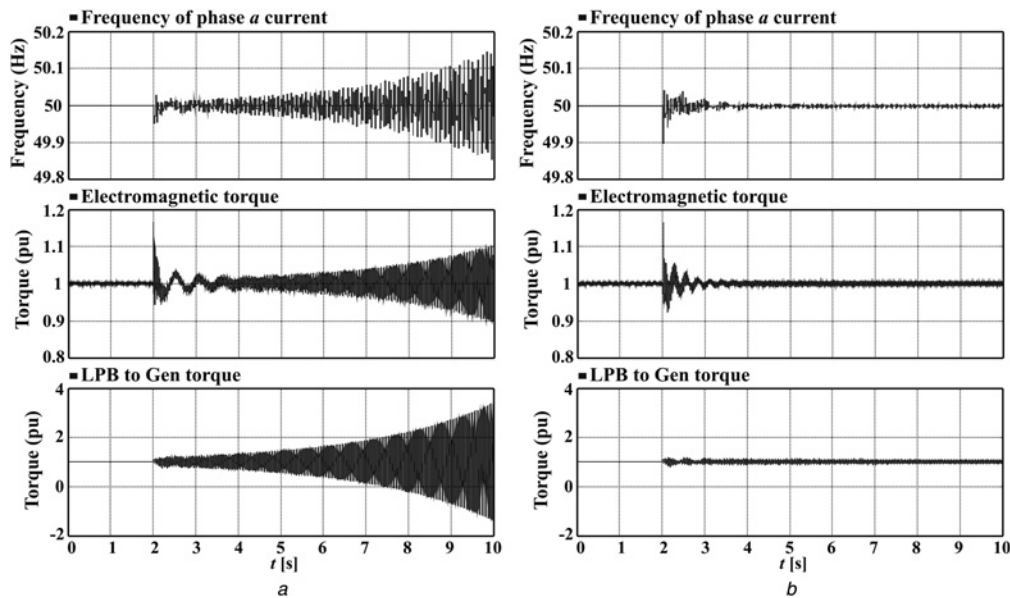


Fig. 8 Experimental results (RTDS signals)

Frequency of phase *a* current, electromagnetic torque, and torque (in the multi-mass shaft between low pressure turbine B and the generator) of the Northern Scotland generator

- a* Damping controller not active
- b* Damping controller active

5 Real-time results

A time domain experiment is carried out on the multi-platform network described by Figs. 6 and 7. In the

first experiment, the damping converter in the VSC-HVDC test rig is not activated. As with the undamped system in Section 3.1, the system develops SSR. This is exhibited through a rising AC system frequency and generator shaft

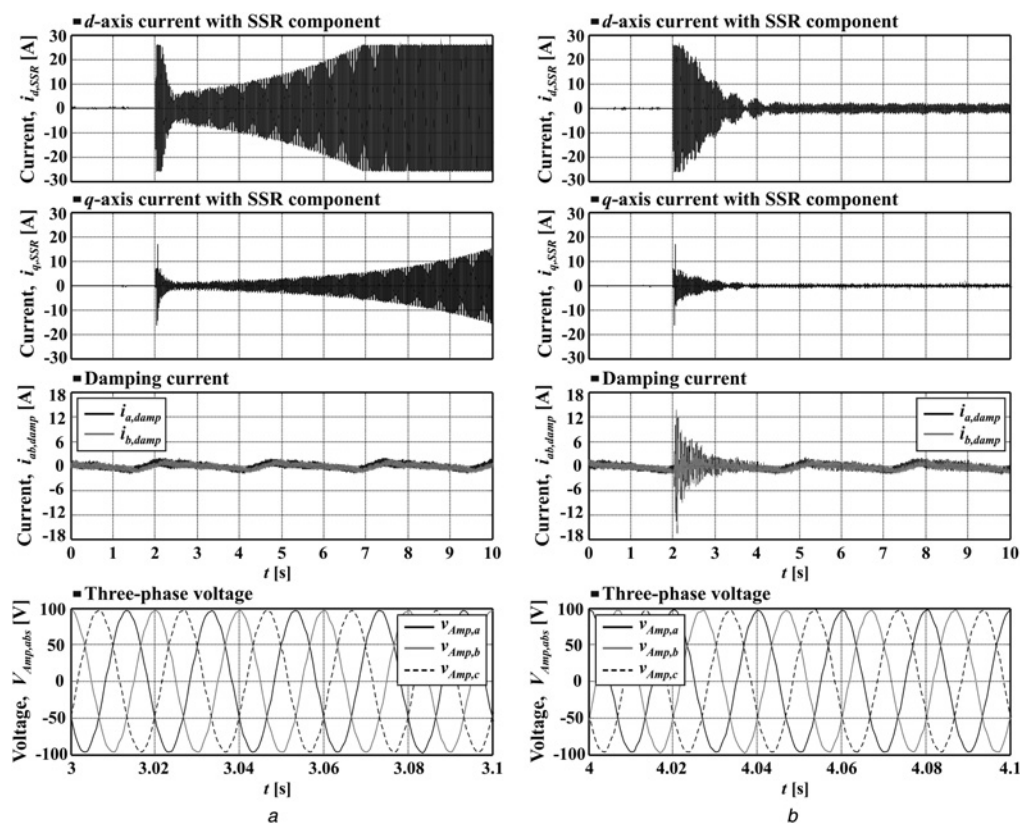


Fig. 9 Experimental results (HVDC rig signals)

dq currents with subsynchronous component coming from RTDS, three-phase damping current from the HVDC (phases *a* and *b*) and three-phase voltage from amplifying converter (zoom in)

- a* Damping controller not active
- b* Damping controller active

torques, as shown in Fig. 8a. These show agreement with Fig. 4a, the simulation undamped case. The results shown in Fig. 9a are from the VSC-HVDC test rig. As SSR develops, the dq SSR current in the damping converter of the HVDC rig increases, with the controller limiting their magnitude to ± 25 A. As in this case the damping control is not activated, when the compensation level is increased at 2 s no damping current is produced by the damping converter, only noise. The voltage produced by the amplifying converter, taken from the Bus 5 voltage on the RTDS, is amplified to the VSC-HVDC rig nominal voltage.

The experiment is repeated with the damping converter on the HVDC-VSC test rig activated, with results shown in Fig. 8b. Following the change of series compensation from 30 to 40% at 2 s, the damping current injected into the AC system prevents SSR from developing. This is shown by the stability of the AC system frequency and torques. Such results are in consistent with those of Fig. 4b. The plots from Fig. 9b demonstrate the behaviour of the VSC-HVDC rig. Initially, the amplitude of the SSR current component is large, but decreases as the SSR is damped. Under normal conditions, the amplitude of the damping current generated by the damping converter is very small and makes no contribution to the AC system. At 2 s the series compensation level is stepped and the damping current increases to counteract the rising SSR current at Bus 5. Although the active and reactive currents are used to damp the SSR, the energy is small as damping is achieved in 1 s. This energy for damping can come from the DC capacitors, minimising the effect on the DC link. The AC voltage provided by the amplifying converter has no variations throughout the change in compensation.

Fig. 10 shows a comparison between the simulation results and experimental results from the RTDS/VSC-HVDC test rig. In Fig. 10a, the undamped cases are compared, with the simulation and real-time experiment showing good agreement. Similarly, Fig. 10b addresses the damped cases; both show good agreement. The improvement in response from the experiment is due to the damper having full control over the active and reactive powers needed to perform damping. In the simulation case, the converter responsible for damping is also maintaining power set points.

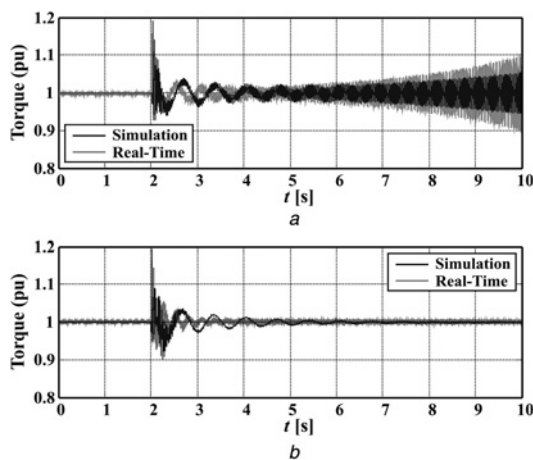


Fig. 10 Comparison of simulation and real-time results
Northern Scotland electromagnetic torque with damping control
a Not active
b Active

6 Conclusions

The proposed reinforcements for the GB transmission network for 2020 include onshore series compensation and offshore HVDC links. The adverse effects in the form of SSR introduced by series compensation in a three-machine network, resembling the operation of the mainland GB system in the 2020, have been examined. Moreover, SSR mitigation has been achieved through a VSC-HVDC link. This has been done both by simulation and through a real-time experiment.

Simulations were carried out in PSCAD/EMTDC software. System analysis was conducted in MATLAB to formally assess SSR occurrence in the three-machine network. The HVDC link was modelled to provide its primary control objective and an auxiliary function for SSR damping. An experiment was undertaken through a hardware-in-the-loop RTDS-HVDC test rig to assess the effectiveness of the proposed damping scheme. Simulation and experimental results showed good agreement.

As VSC-HVDC converters are utilised more in the future, their flexibility can be used to damp power system oscillations in adjacent AC transmission systems. This may be cost effective by eliminating the requirement for additional power electronics equipment (such as TCSCs).

7 Acknowledgement

This work was supported by the Engineering and Physical Sciences Research Council (EPSRC), Research Councils U.K. (RCUK), under Grant ‘‘Centre for Integrated Renewable Energy Generation and Supply (CIREGS),’’ number EP/E036503/1. J. Ekanayake’s work was supported in part by the Low Carbon Research Institute (LCRI). Q. Mu’s work was supported by the National Natural Science Foundation under the project 51128701.

8 References

- 1 National Grid: ‘GB Seven Year Statement’, 2010. Available from: <http://www.nationalgrid.com/uk/Electricity/SYS/>, accessed January 2013
- 2 Electricity Networks Strategy Group (ENSG): ‘Our Electricity Transmission Network: a Vision for 2020’, 2012. Available from: <http://www.decc.gov.uk/assets/decc/11/meeting-energy-demand/future-electric-network/4263-ensgFull.pdf>, accessed January 2013
- 3 Hor, C., Finn, J., Thumm, G., Mortimer, S.: ‘Introducing series compensation in the UK transmission network’. IET ACDC, 2010, pp. 1–5
- 4 Anderson, P.M., Agrawal, B.L., Van Ness, J.E.: ‘Subsynchronous resonance in power systems’ (IEEE Press, USA, 1990)
- 5 Subsynchronous Resonance Working Group: ‘Reader’s guide to subsynchronous resonance’, *IEEE Trans. Power Syst.*, 1992, 7, (1), pp. 150–157
- 6 Farmer, R.G., Schwalb, A.L., Katz, E.: ‘Navajo project report on subsynchronous resonance analysis and solutions’, *IEEE Trans. Power Appar. Syst.*, 1977, 96, (4), pp. 1226–1232
- 7 Kundur, P.: ‘Power systems stability and control’ (McGraw-Hill, USA, 1994)
- 8 IEEE Subsynchronous Resonance Task Force: ‘First benchmark model for computer simulation of subsynchronous resonance’, *IEEE Trans. Power Appar. Syst.*, 1977, 96, (5), pp. 1565–1572
- 9 Hall, M.C., Hodges, D.A.: ‘Experience with 500 kV subsynchronous resonance and resulting turbine generator shaft damage at Mohave generating station’. Proc. IEEE PES Winter Meeting, 1976, pp. 22–30
- 10 Hughes, F.M., Anaya-Lara, O., Jenkins, N., Strbac, G.: ‘A power system stabilizer for DFIG-based wind generation’, *IEEE Trans. Power Syst.*, 2006, 21, (2), pp. 763–772
- 11 Hingorani, N.G., Bhargava, B., Garrigue, G.F., Rodriguez, G.D.: ‘Prototype NGH subsynchronous resonance damping scheme part I – field installation and operating experience’, *IEEE Trans. Power Syst.*, 1987, 2, (4), pp. 1034–1039

- 12 IEEE Subsynchronous Resonance Working Group: 'Countermeasures to subsynchronous resonance problems', *IEEE Trans. Power Appar. Syst.*, 1980, **99**, (5), pp. 1810–1818
- 13 Patil, K.V., Senthil, J., Jiang, J., Mathur, R.M.: 'Application of STATCOM for damping torsional oscillations in series compensated AC systems', *IEEE Trans. Energy Convers.*, 1998, **13**, (3), pp. 237–243
- 14 Iravani, M.R., Mathur, R.M.: 'Damping subsynchronous oscillations in power systems using a static phase-shifter', *IEEE Trans. Power Syst.*, 1986, **1**, (2), pp. 76–82
- 15 Hedin, R.A., Weiss, S., Torgerson, D., Eilts, L.E.: 'SSR characteristics of alternative types of series compensation schemes', *IEEE Trans. Power Syst.*, 1995, **10**, (2), pp. 845–852
- 16 Zhu, W., Spee, R., Mohler, R.R., Alexander, G.C., Mittelstadt, W.A., Maratukulam, D.: 'An EMTF study of SSR mitigation using the thyristor controlled series capacitor', *IEEE Trans. Power Deliv.*, 1995, **10**, (3), pp. 1479–1485
- 17 Pilotto, L.A.S., Bianco, A., Long, W.F., Edris, A.A.: 'Impact of TCSC control methodologies on subsynchronous oscillations', *IEEE Trans. Power Deliv.*, 2003, **18**, (1), pp. 243–252
- 18 National Grid: 'NETS Security and Quality of Supply Standard. Issue 2.2', 2012. Available from: <http://www.nationalgrid.com/uk/Electricity/Codes/gbsqsscode/DocLibrary/>, accessed January 2013
- 19 Dodds, S., Railing, B., Akman, K., Jacobson, B., Worzyk, T., Nilsson, B.: 'HVDC VSC (HVDC light) transmission – operating experiences'. Proc. CIGRE Session, Paris, France, 2010, pp. 1–9
- 20 Hamouda, R.M., Iravani, M.R., Hackam, R.: 'Torsional oscillations of series capacitor compensated AC/DC systems', *IEEE Trans. Power Syst.*, 1989, **4**, (3), pp. 889–896
- 21 Hsu, Y.Y., Wang, L.: 'Modal control of an HV DC system for the damping of subsynchronous oscillations', *IEE Proc. – Gener. Transm. Distrib.*, 1989, **136**, (2), pp. 78–86
- 22 Livermore, L., Ugalde-Loo, C.E., Liang, J., Ekanayake, J.B., Jenkins, N.: 'Damping of subsynchronous resonance using a VSC-HVDC link'. Proc. 17th Power Systems Computation Conf. (PSCC), Stockholm, Sweden, 22–26 August, 2011, pp. 1–7
- 23 Ugalde-Loo, C.E., Ekanayake, J.B., Jenkins, N.: 'Subsynchronous resonance in a series compensated Great Britain transmission network', *IET Gener. Transm. Distrib.*, 2013, **7**, (3), pp. 209–217
- 24 Ugalde-Loo, C.E., Ekanayake, J.B., Jenkins, N.: 'Subsynchronous resonance on series compensated transmission lines with quadrature boosters'. Proc. IEEE PES PowerTech 2011, Trondheim, Norway, 19–23 June, 2011, pp. 1–7
- 25 Irwin, G.D., Jindal, A.K., Isaacs, A.L.: 'Sub-synchronous control interactions between type 3 wind turbines and series compensated AC transmission systems'. 2011 IEEE Proc. Power and Energy Society General Meeting, 24–29 July 2011, pp. 1–6
- 26 Flourentzou, N., Agelidis, V.G., Demetriades, G.D.: 'VSC-based HVDC power transmission systems: an overview', *IEEE Trans. Power Electron.*, 2009, **24**, (3), pp. 592–602
- 27 Bresesti, P., Kling, W.L., Hendriks, R.L., Vailati, R.: 'HVDC connection of offshore wind farms to the transmission system', *IEEE Trans. Energy Convers.*, 2007, **22**, (1), pp. 37–43
- 28 Prabhu, N., Padiyar, K.R.: 'Investigation of subsynchronous resonance with VSC-based HVDC transmission systems', *IEEE Trans. Power Deliv.*, 2009, **24**, (1), pp. 433–440
- 29 Liang, J., Jing, T.J., Gomis-Bellmunt, O., Ekanayake, J., Jenkins, N.: 'Operation and control of multiterminal HVDC transmission for offshore wind farms', *IEEE Trans. Power Deliv.*, 2011, **26**, (4), pp. 2596–2604
- 30 Liang, J., Gomis-Bellmunt, O., Ekanayake, J., Jenkins, N., An, W.: 'A multi-terminal HVDC transmission system for offshore wind farms with induction generators', *Int. J. Electr. Power Energy Syst.*, 2012, **43**, (1), pp. 54–62
- 31 Department of Energy and Climate Change (DECC): 'The impact of changing energy use patterns in buildings on peak electricity demand in the UK', 2008. Available from: <http://www.decc.gov.uk/assets/decc/11/about-us/science/3150-final-report-changing-energy-use.pdf>, accessed January 2013

9 Appendix 1: three-machine system [23]

Machine rating: Southern Scotland: 2800 MVA, 33 kV. Northern Scotland: 2400 MVA, 33 kV. England and Wales: 21 000 MVA, 400 kV. Base frequency: $f_b = 50$ Hz, $\omega_b = 2\pi f_b$.

The following parameters are given in pu unless stated otherwise.

Synchronous generators (on base of machine rating): $R_a = 0.002$, $X_l = 0.17$, $X_q = 2.07$, $X'_q = 0.906$, $X''_q = 0.234$, $X_d = 2.13$, $X'_d = 0.308$, $X''_d = 0.234$, $X_{mq} = 1.9$, $X_{md} = 1.96$, $\tau_{d0} = 6.0857$ s, $\tau'_{d0} = 1.653$ s, $\tau''_{d0} = 0.0526$ s and $\tau'_{q0} = 0.3538$ s. Rotor windings parameters are calculated as in [7].

Single-mass shaft (Southern Scotland and England/Wales generators): Inertias (MWs/MVA): $H_{SScot} = 3.84$, $H_{EW} = 5$. Damping coefficients (pu T/pu speed dev.): $D_{SScot} = D_{EW} = 0.1$.

Multi-mass shaft (Northern Scotland generator): Inertias (in MWs/MVA): $H_H = 0.092897$, $H_I = 0.155589$, $H_{LA} = 0.858670$, $H_{LB} = 0.884215$, $H_G = 0.868495$ and $H_X = 0.0342165$. Self and mutual damping coefficients (in pu T/pu speed dev.): $D_H = D_I = D_{LA} = D_{LB} = 0.1$, $D_G = D_X = 0$, $D_{HI} = D_{IA} = D_{AB} = D_{BG} = 0.2$, $D_{GX} = 0.005$. Torsional stiffness (in pu T/rad): $K_{HI} = 19.303$, $K_{IA} = 34.929$, $K_{AB} = 52.038$, $K_{BG} = 70.858$, $K_{GX} = 2.822$.

Transformers (on a 1000 MVA base): $X_{11} = 0.14$, $X_{21} = 0.07$.

Transmission lines (on a 1000 MVA base): $X_{12} = 0.01$, $X_{22} = 0.1$, $X_3 = 0.05$. A ratio $X/R = 10$ is assumed. Shunt capacitances $X_{CSh} = 20$ pu are considered for the π representations.

Loads (on a 1000 MVA base): $P_{L3} = 17.73$, $Q_{L3} = 2.4847$. $P_{L4} = 2.0$, $Q_{L4} = 0$.

10 Appendix 2: simulation and VSC-HVDC rig control parameters

10.1 Self-contained simulation

Primary controller

Active power: $K_{PI} = 0.0001$, $\tau_{PI} = 0.05$. **Reactive power:** $K_{PI} = 0.01$, $\tau_{PI} = 0.5$. I_d current: $K_{PI} = -0.5$, $\tau_{PI} = 0.003$. I_q current: $K_{PI} = 2.5$, $\tau_{PI} = 0.01$. **DC voltage:** $K_{PI} = 0.02$, $\tau_{PI} = 0.8$. **Reactive power 2:** $K_{PI} = -0.1$, $\tau_{PI} = 0.001$. I_d current: $K_{PI} = 0.5$, $\tau_{PI} = 0.005$. I_q current: $K_{PI} = -0.1$, $\tau_{PI} = 0.001$.

Auxiliary controller

BPF: centre frequency: 20 Hz, **Lead-lag compensator:** gain $K_{L-L} = 10$, time constants $\tau_{Lead} = 0.004$, $\tau_{Lag} = 0.009$.

10.2 RTDS/VSC-HVDC experimental platform

Damping controller: **HPF:** cut-off frequency 15 Hz, 4 pole-pairs. **LPF:** cut-off frequency 25 Hz, 4 pole-pairs. **Lead-lag comp. (trans.):** $K_{L-L} = 5$, $\tau_{Lead} = 0.0428$, $\tau_{Lag} = 0.015$. **Scaling (trans.):** RTDS \rightarrow HVDC current factor 4, voltage factor 400. HVDC \rightarrow RTDS current factor 16. **Lead-lag comp. (damp.):** $K_{L-L} = 5$, $\tau_{Lead} = 0.0042$, $\tau_{Lag} = 0.0096$.

11 Appendix 3: RTDS and VSC-HVDC rig hardware parameters

VSCs: Operated power 1 kW, AC voltage 120 V, DC voltage 250 V. **Topology:** Two level, 3- ϕ without neutral wire.

AC Inductors: $L_{AC} = 2.2$ mH. **DC Inductors:** $L_{DC} = 2.4$ mH, $R_{eq} = 0.15$ Ω . **DC Capacitor:** $C = 1020$ μ F.

dSPACE model: DS1005.

RTDS Racks: 1. **Cards:** 1 GTWIF, 4 GPC (2 IBM PPC750GX 1 GHz), 1 GTIRC, 1 GTDI, 1 GTDO, 1 GTAI, 1 GTAO, 1 GTNET.